Mathematical Modelling and Numerical Simulation with Applications, 2023, 3(4), 376–390

https://dergipark.org.tr/en/pub/mmnsa
ISSN Online: 2791-8564 / Open Access
https://doi.org/10.53391/mmnsa.1398320

RESEARCH PAPER

The role of calcium dynamics with amyloid beta on neuron-astrocyte coupling

Hemlata Jethanandani [1,‡], **Brajesh Kumar Jha** [2,*,‡] **and Manisha Ubale** [1,‡]

[1]Department of Science & Humanities, Indus Institute of Science Humanities & Liberal Studies (IISHLS), Indus University Rancharda, Ahmedabad-382115 Gujarat, India, [2]Department of Mathematics, School of Technology, Pandit Deendayal Energy University, Gandhinagar 382426, Gujarat, India

*Corresponding Author
‡ hemlatajethanandani.rs@indusuni.ac.in (Hemlata Jethanandani); brajesh.jha@sot.pdpu.ac.in (Brajesh Kumar Jha); manishadalbhide.gen@indusuni.ac.in (Manisha Ubale)

Abstract

Amyloid beta ($A\beta$) plaques are associated with neurodegenerative diseases such as Alzheimer's disease. Due to the involvement of $A\beta$ plaques in the functioning of the brain; cognitive decline disrupts calcium homeostasis in nerve cells and causes abnormal calcium ions (Ca^{2+}) signaling patterns. In consequence, there is enhanced neuronal excitability, compromised synaptic transmission, and decreased astrocytic function. Neuron-astrocyte coupling through calcium dynamics with different neuronal functions has been studied. Key signaling molecules in this process include Ca^{2+}, which control several cellular functions, including neurotransmission and astrocytic regulation. The mathematical model for neuron-astrocyte communication has been developed to study the importance of calcium dynamics in signal transduction between the cells. To understand the wide role of mitochondria, NCX, and amyloid beta with various necessary parameters included in the model, Ca^{2+} signaling patterns have been analyzed through amplitude modulation and frequency modulation. The results of the current model are simulated and analyzed using XPPAUT. The findings of the current study are contrasted with experimental data from an existing mathematical model that illustrates the impact of calcium oscillation frequency and amplitude modulations in nerve cells.

Keywords: Neuron; astrocytes; neurodegenerative diseases; calcium dynamics; amyloid beta

AMS 2020 Classification: 37M05; 00A71; 34D20

1 Introduction

Amyloid beta ($A\beta$) builds up in the brain and causes progressive cognitive impairment, which are hallmarks of Alzheimer's disease (AD), a debilitating neurodegenerative condition [1]. The

➤ **Received:** 30.11.2023 ➤ **Revised:** 27.12.2023 ➤ **Accepted:** 29.12.2023 ➤ **Published:** 30.12.2023

complex interplay between $A\beta$ and calcium dynamics in neurons and astrocytes has been brought to light by recent studies [2]. Maintaining brain homeostasis depends on the neuron-astrocyte connection, and disruptions in calcium signaling are linked to the etiology of AD. Neuronal dysfunction and cell death in AD are believed to be profoundly influenced by the disruption of Ca^{2+} homeostasis [3]. Maintaining appropriate Ca^{2+} levels requires neuron-astrocyte interaction, and recent studies have shown the importance of mitochondria and NCX in this process [4].

In order to control Ca^{2+} signaling, these two cell types engage in intricate interactions known as neuron-astrocyte coupling [5]. Through specialised transporters, astrocytes absorb excess synaptic Ca^{2+}, thereby buffering Ca^{2+} levels in neurons and reducing excitotoxicity [6]. By compromising astrocytic Ca^{2+} regulation, $A\beta$ has been demonstrated to interfere with this coupling and increase neuronal susceptibility to Ca^{2+} overload [5].

An essential function of mitochondria is to preserve the Ca^{2+} homeostasis of neurons and astrocytic membranes [7]. Research has indicated that an accumulation of $A\beta$ within mitochondria can impair their functionality and result in a higher generation of reactive oxygen species (ROS). Due to decreased mitochondrial Ca^{2+} buffering, which lowers the effectiveness of Ca^{2+} clearance within neurons and astrocytes, this mitochondrial dysfunction can cause problems with Ca^{2+} handling [8].

Apart from their function of buffering Ca^{2+}, mitochondria also use processes like Ca^{2+} absorption and release to modify Ca^{2+} signalling. These mechanisms can be changed by $A\beta$-induced mitochondrial dysfunction, which can impact the Ca^{2+} dynamics in neurons and astrocytes [9, 10]. Uncontrolled release of Ca^{2+} by malfunctioning mitochondria can lead to astrocytic dysfunction and neuronal excitotoxicity [11, 12]. In neurons and astrocytes, the sodium-calcium exchanger (NCX) plays a critical role in controlling intracellular Ca^{2+} levels [13]. It has been demonstrated that $A\beta$ disrupts NCX function by changing its expression and activity [14]. Further altering neuron-astrocyte connection, dysregulated NCX can worsen Ca^{2+} dysregulation by increasing Ca^{2+} inflow and impairing Ca^{2+} extrusion in both cell types [2]. The two main cell types in the central nervous system are neurons and astrocytes, and the proper functioning of these two populations is essential for brain maintenance [15]. Key signaling molecules, such as calcium ions Ca^{2+}, are involved in several cellular activities, such as neurotransmitter release, plasticity, and synaptic transmission. Calcium signaling is a mechanism used by both neurons and astrocytes to exchange information and react to modifications in the brain's microenvironment [16]. Action potentials are produced when neurons release neurotransmitters into the synaptic cleft, which causes postsynaptic calcium influx [17]. Changes in synaptic activity and calcium levels are actively sensed by astrocytes, which surround synapses with their tiny processes. Astrocytes can control neuronal excitability and synaptic transmission through a process called gliotransmission [15].

Amyloid beta and calcium de-regulation $A\beta$, the pathogenic hallmark protein in AD, has been shown to disrupt calcium homeostasis in neurons and astrocytes, with important effects for neuron-astrocyte connection [18]. $A\beta$ peptides have direct interactions with ion channels, including those that control calcium levels, and cell membranes. Increased intracellular calcium levels in neurons as a result of this interaction ultimately cause neuronal death, and synaptic dysfunction [1, 11]. Astrocytic calcium dynamics are similarly impacted by $A\beta$ exposure. The removal of extracellular $A\beta$ is mostly dependent on astrocytes, and an elevated $A\beta$ load may cause abnormal calcium signaling in astrocytes. Dysfunctional astrocytic calcium signaling undermines their ability to support neurons, compromising synaptic function and neuronal survival [1, 12, 19]. Normally, astrocytes remove excess glutamate from synapses to avoid excitotoxicity. This function is compromised by $A\beta$-induced disturbances in astrocytic calcium signaling, which prolong glutamate exposure at synapses [4].

Neurotransmission is impacted by changes in calcium dynamics in both astrocytes and neurons.

Reduced synaptic effectiveness and aberrant synaptic plasticity can be caused by $A\beta$-mediated dysregulation [13, 16]. In astrocytes, dysregulation of calcium induced by $A\beta$ can exacerbate neuroinflammation. The neurodegenerative process is accelerated by reactive astrocytes that emit proinflammatory cytokines. The complex interactions among $A\beta$, mitochondria, NCX, and neuron-astrocyte coupling have a major effect on the dynamics of Ca^{2+} in AD. By upsetting the delicate balance of Ca^{2+} homeostasis, $A\beta$ causes malfunction in the mitochondria, interferes with NCX activity, and affects astrocytic Ca^{2+} regulation. The pathogenesis of AD is aided by these consequences, which increase neuronal susceptibility to Ca^{2+} excess. In order to determine viable therapeutic strategies targeted at reestablishing appropriate Ca^{2+} homeostasis in Alzheimer's disease, future research should carry out an exploration of these pathways [20].

We offer a theoretical framework in this work to understand the driving forces behind different Ca^{2+} oscillation patterns in an AD environment. Examining model solutions additionally provides valuable insights into how $A\beta$ affects Ca^{2+} basal levels across a range of timescales. Numerous studies have been conducted on calcium dynamics to illustrate the impacts of different parameters, as evidenced by the literature review. Parkinson's disease starts to progress early when there is a loss or change in this cellular activity [21–23]. To analyze the spatiotemporal fluctuations of intracellular Ca^{2+} concentration in T lymphocyte cells, a two-dimensional mathematical model has been explored [24]. During oocyte development, eggs develop the capacity to create this specific calcium transient. It has been demonstrated that oocyte cells exhibit cytosolic calcium signaling through the use of parameters including buffers, ryanodine receptor (RyR), and Serca pump [25, 26]. Understanding the cellular mechanism underlying the inclusion and extrusion of free calcium is essential [27]. It has been demonstrated analytically and quantitatively how the glycolytic oscillator chemical model behaves through the flip and generalized flip bifurcations [28].

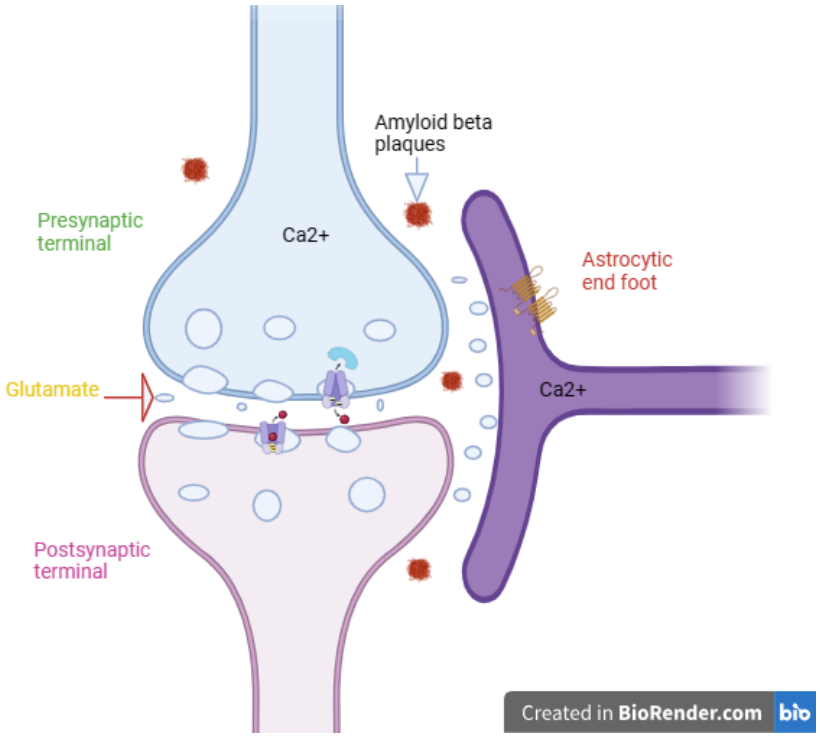

Figure 1. Neuron-astrocyte signaling

2 Mathematical model of the problem

Neuron model

The leaky integrate and fire model (LIF) has been used to show the neural communication with required parameters [2]:

$$\tau_m \frac{dV(t)}{dt} = -V(t) + R_m I_{syn}, \tag{1}$$

where V is the membrane voltage, R_m is the membrane resistance, I_{syn} is the input current, and τ_m is the membrane time constant. V is clamped at $0V(volt)$ when the neuron membrane potential (V) approaches a firing threshold value for the neuron, (V_{th}).

Astrocyte-neuron interactions

Gliotransmitters that change neurotransmitter reuptake, boost synaptic strength, or control pruning of synaptic cells may be emitted by astrocytes when exposed to an action potential from a neuron. The neuron-astrocyte coupling process for Ca^{2+} dynamics is heavily dependent on the inositol trisphosphate (IP_3) signaling pathway. Neurotransmitters released by stimulated neurons can activate receptors on astrocytes. The activation of these receptors results in the synthesis of IP_3, a secondary messenger molecule that causes the astrocyte's internal stores of Ca^{2+} to be released. Surrounding neurons may be profoundly impacted by this Ca^{2+} increase in astrocytes, which can alter their activity and synaptic transmission. The model states that the extent of neurotransmitter exposure affects the extension of IP_3. The neuron-astrocyte coupling describes the two-way exchange of information and interaction that occurs between astrocytes and neurons [29, 30].

$$\frac{dIP_3}{dt} = \frac{IP_3^* - IP_3}{\tau_{ip_3}} + r_{ip_3(AG)}, \tag{2}$$

where r_{ip_3} is the IP_3 assembly rate, IP_3^* is the baseline of IP_3 in the steady-state,τ_{ip_3} is the IP_3 decay rate.

Astrocyte dynamics

The Ca^{2+} flux inside the astrocyte is measured using the Li-Rinzel model. Many computational simulations inside the Li-Rinzel model have demonstrated Ca^{2+} oscillations for a range of parameter settings [31]. The intracellular expansion triggers reactions in the cytosolic calcium absorption process, including the ER leakage flux, the pump-flux from the cytosol into the ER, and the Ca^{2+} flux from the ER(Endoplasmic Reticulum) over the IP_3 carriers. By moving Ca^{2+} across the plasma membrane, the Na^+/Ca^{2+} exchanger influences the intracellular Ca^{2+} concentration. The differential equation for the dynamics of Ca^{2+} in mitochondria is governed by a balance of Ca^{2+} fluxes [2, 32]:

$$\frac{d\left[Ca^{2+}\right]}{dt} = J_{channel} - J_{pump} + J_{leak} + J_{in} - J_{out} - J_{MCU} + J_{mNCX} - J_{NCX}, \tag{3}$$

$$\frac{dh}{dt} = \frac{h_\infty - h}{\tau_h}, \tag{4}$$

where

$$h_\infty = \frac{Q_2}{Q_2 + Ca^{2+}}, \tag{5}$$

$$\tau_h = \frac{1}{a_2 \left(Q_2 + Ca^{2+}\right)}, \tag{6}$$

$$Q_2 = d_2 \frac{IP_3 + d_1}{IP_3 + d_3}, \tag{7}$$

where h is the fraction of activated IP_3. The following calculates the calcium flux via the channel, pump-flux, and leakage flux from the ER:

$$J_{pump} = v_{ER} \left(\frac{\left(Ca^{2+}\right)^2}{k_{ER}^2 + \left(Ca^{2+}\right)^2} \right), \tag{8}$$

$$J_{chan} = r_c m_\infty^3 n_\infty^3 h^3 \left(c_0 - (1 + c_1) \, Ca^{2+} \right), \tag{9}$$

$$J_{leak} = r_L \left(c_0 - (1 + c_1) \, Ca^{2+} \right), \tag{10}$$

$$J_{out} = k_1 Ca^{2+}, \tag{11}$$

$$J_{NCX} = c_0 \left(\frac{Na_i}{Na_0} \right)^3 exp \left(\frac{2FV_m}{RT} \right), \tag{12}$$

with

$$m_\infty = \frac{IP_3}{IP_3 + d_1}, \tag{13}$$

$$n_\infty = \frac{Ca^{2+}}{Ca^{2+} + d_5}, \tag{14}$$

where r_c represents the maximum CICR (Calcium-induced calcium release) rate, c_0 represents the total of the free Ca^{2+} cytosolic collection, and c_1 represents the ER/cytoplasm capacity ratio. The IP_3 induced calcium release is shown by m_∞, the CICR channels are indicated by n_∞, the maximum absorption amount for the SERCA pump is v_{ER}, the stimulation constant of the SERCA pump is k_{ER}, and the calcium leakage amount is r_L.

Amyloid beta hypothesis

IP_3 concentration is modeled as a linearly increasing function of the membrane leak J_{in}. To ensure that the steady-state Ca^{2+} concentration relies on p, we only include a linearly increasing contribution in this case, even if this rise could be the result of many causes. The effects of $A\beta$ on the existence of exchangers, channels, and pumps are still largely unknown. Despite this, we have used some of the offered papers to view the $A\beta$ influence. To add $k_\beta a^m$ in J_{in} in order to account for the effect of $A\beta$ in the model [6, 30]:

$$J_{in} = a_1 + a_2 p + k_\beta a^m, \tag{15}$$

where a_1 and a_2 are parameters and m denotes a cooperatively coefficients and k_β is a constant of speed.

Mitochondria model

Studies have demonstrated that the ER and mitochondria cooperate to generate complex functional membranes associated with the ER that is mitochondria-associated membranes (MAMs). The Ca^{2+} concentration between ER-Mitochondria can reach 10 times higher integrity than in the bulk cytoplasm when cells are activated. When properly activated, the mitochondrial Ca^{2+} uniporter (MCU) allows for an increase in Ca^{2+} levels [33]. Owing to their bidirectional nature, the local Ca^{2+} intake by mitochondria and the inositol triphosphate receptor (IP_3R) by Ca^{2+} can both expand or contract the ER. Ca^{2+} reveals that by severing the effective feedback from Ca^{2+} on IP_3R, Ca^{2+} releases, by reducing the ER or the Ca^{2+}-related IP_3Rs deactivation [7, 8, 34]:

$$\frac{d\left[Ca^{2+}\right]_{Mt}}{dt} = J_{MCU} - J_{mNCX}, \tag{16}$$

$$J_{MCU} = v_{mNCX}\left(\frac{Na^3}{k_{Na}^3 + Na^3}\right)\left(\frac{\left[Ca^{2+}\right]_{Mt}}{k_{mNCX} + \left[Ca^{2+}\right]_{Mt}}\right), \tag{17}$$

$$J_{mNCX} = v_{MCU}\left(\frac{\left[Ca^{2+}\right]^2}{k_{MCU}^2 + \left[Ca^{2+}\right]^2}\right), \tag{18}$$

where $\left[Ca^{2+}\right]_{Mt}$ mitochondrial calcium concentration and J_{MCU} and J_{mNCX} are fluxs of Ca^{2+} ions through the mitochondrial Ca^{2+} uniporter and mNCX channels.

Endocannabinoid dynamics

Several computational models represent the interaction between astrocytes and neurons using tripartite synapse connections. When the signal-receiving neuron is sufficiently depolarized and the synaptic cleft releases a glutamate-like neurotransmitter, 2-AG leaves from the dendrite and attaches itself to CB1Rs on the surface of astrocytes [2]. The model equations are

$$\frac{d\left(AG\right)}{dt} = -\frac{AG}{\tau_{AG}} + r_{AG}H\left(c - c_{th}\right), \tag{19}$$

$$\frac{d\,(Glu)}{dt} = -\frac{Glu}{\tau_{Glu}} + r_{Glu} H\,(c - c_{th})\,, \tag{20}$$

where AG denotes the quantity of 2-AG and Glu denotes the amount of glutamate, and τ_{AG} and τ_{glu} indicate the relaxation time constants for 2-AG and glutamate, respectively. Glutamate release and 2-AG production are denoted by the variables r_{AG} and r_{Glu}, respectively. The release of 2-AG and glutamate is indicated by the Heaviside function $H(c - c_{threshold})$, which is accompanied by the Ca^{2+} threshold and catalyzed by calcium [27].

Table 1. Values of biophysical parameters

Astrocyte Constraint	Constraint Description	Value
τ_{AG}	Decay rate of 2-AG	10 s
τ_{Glu}	Decay rate of Glutamate	100 ms
r_{Glu}	Maximum rate of Glutamate production	10 μMs^{-1}
r_{AG}	Maximum rate of AG production	0.018 μMs^{-1}
IP_3^*	Baseline value of IP_3	0.16 μM
r_{IP_3}	Rate of IP_3 production	0.5 μMs^{-1}
r_C	Maximum rate of CICR	6 s^{-1}
r_L	Ca^{2+} leakage rate from ER	0.11 s^{-1}
v_{ER}	Maximum rate of SERCA uptake	0.8 μMs^{-1}
k_{ER}	SERCA pump activation constant	0.1 μM
c_1	Ratio of ER volume to cytosol volume	0.185
d_1	IP_3 Disconnection constant Ca^{2+}	0.13 μM
d_2	Ca^{2+} Dismissal dissociation constant Ca^{2+}	1.049 μM
d_3	IP_3 Separation constant Ca^{2+}	0.9434 μM
d_5	Ca^{2+} Stimulate dissociation constant Ca^{2+}	0.08234 μM
a_2	IP3R Ca^{2+} Dismissal binding rate	0.2 μMs^{-1}
$Ca^{2+}threshold$	Astrocyte Glutamate release threshold	0.3 μM
c_0	Total free Ca^{2+} cytosol concentration	2 μM
τ_m	Membrane time constant	0.1
I_{sym}	Injected current	2
V	Firing threshold voltage	9 mv
R_m	Membrane resistance	1.2 $G\Omega$
k_{Na}	Na^+ activation constants for the mNCX	7.4 mM
k_{mNCX}	Ca^{2+} activation constants for mNCX	45 μM
k_{MCU}	Ca^{2+} activation constants for MCU	0.84 μM
Na^+	Na^+ Concentrations in the Cytosol	12 mM
V_{mNCX}	Maximal flux through the mNCX	100 μMs^{-1}
V_{MCU}	Maximal flux through the MCU	0.07 μMs^{-1}
Na_i	Intracellular Na^+ concentration	12 μM
Na_o	Extracellular Na^+ concentration	145 μM
F	Faraday's constant	96485 $Cmol^{-1}$
R	Gas constant	8.314 $JK^{-1}mol^{-1}$
T	Absolute temperature	310 (^oC)
V_m	Membrane potential	-70000 V
k_1	Rate constant of Ca^{2+} extrusion	0.5 s^{-1}
a_1	Parameter for membrane leak	0.1 μMs^{-1}
a_2	Parameter for membrane leak	0.02 s^{-1}
k_β	Constant of speed	0.18 s^{-1}
m	Cooperatively coefficients	4
p	Linear increase of IP_3	0.13
a	Measurement of $A\beta$ presence	1.15

Table 1 provides the starting values for the variables and parameters used in this work [2, 33–35]. The system appears to be inactive based on the principal variable rates. By initializing both variables to zero, experimental measurements have been made for Ca^{2+} and h. To duplicate the model, IP_3 levels have been limited at $0.16\mu M$ (that is equal to IP_3^*) until Ca^{2+} and h have been balanced [36–38].

3 Results

The mechanism of Ca^{2+}-dependent exosome release is examined, along with the coupling of neuron and astrocytes on the Ca^{2+}-driven exosomal dynamics, in response to different values of factors linked to mitochondria, NCX, and amyloid beta. The parameter values listed in Table 1 are used to generate the numerical results provided in this section [2, 33–35]. We aim to demonstrate the influence of $A\beta$ on the promotion of a chemical involved in several cellular processes. As of right now, IP_3 serves as the main agonist, which can subsequently cause the release of Ca^{2+} from different fluxes. In all figures, c represents Ca^{2+} concentrations.

i. First, we have used the neglected NCX (Sodium-Calcium exchanger) and Amyloid beta effects on Ca^{2+} dynamics to characterize the model's solutions with mitochondria.
ii. Secondly, we have extended to incorporate the impact of NCX (sodium-calcium exchanger) on neuron-astrocyte coupling calcium dynamics, likewise in the absence of amyloid beta.
iii. Finally, we have incorporated flux J_{in} to account for the $A\beta$ impacts of membrane potential on Ca^{2+} dynamics.

The neuron-astrocyte model has been analyzed using the XPPAUT software, and the Euler integration approach was employed in all of the results shown here. The model dynamics in the following three sections demonstrate that aberrant Ca^{2+} can arise when $A\beta$ is present. These aberrant signals can arise in a variety of scenarios, pointing to a complex relationship between $A\beta$'s effect and the model's constituent parts. As a result, we deconstruct the model's dynamics by monitoring the outcomes of changing one or two parameters inside a particular signaling component. Finally, we take membrane potential into account and explore model solutions at different $A\beta$ levels while IP_3 concentration is fixed [39].

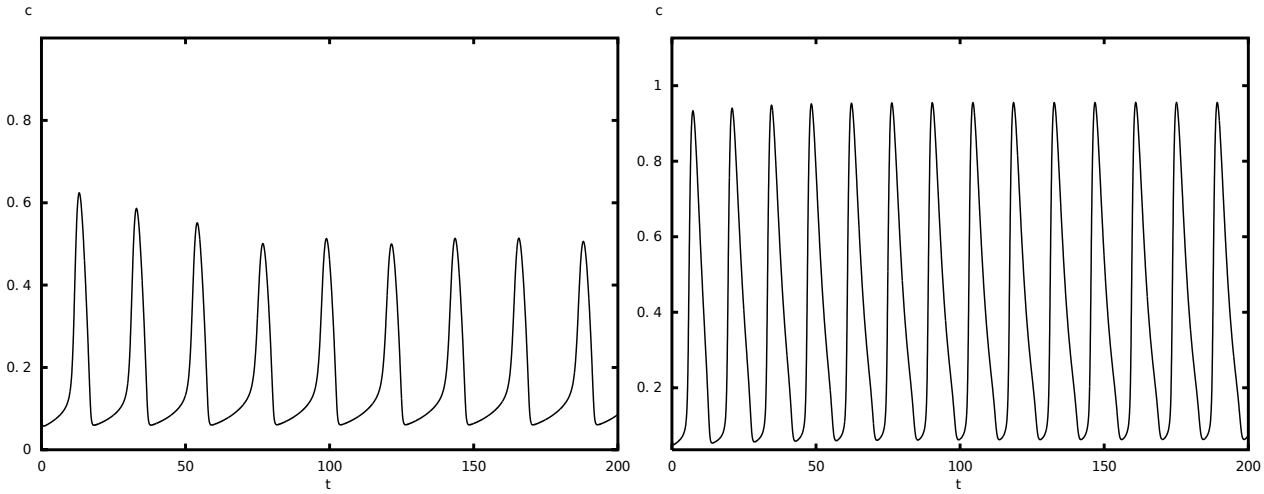

Figure 2. The Ca^{2+} frequency modulation is displayed in Figure 2(a)-Figure 2(b). Figure 2(a) displays the FM mode results of Ca^{2+} oscillations for $r_L = 0.11$, $IP_3 = 0.29$, and $k_{ER} = 0.09$ in the proposed model while Figure 2(b) displays the FM mode results of Ca^{2+} oscillations for $r_L = 0.8$, with fixed values of $IP_3 = 0.78$ and $k_{ER} = 0.07$ in the original model

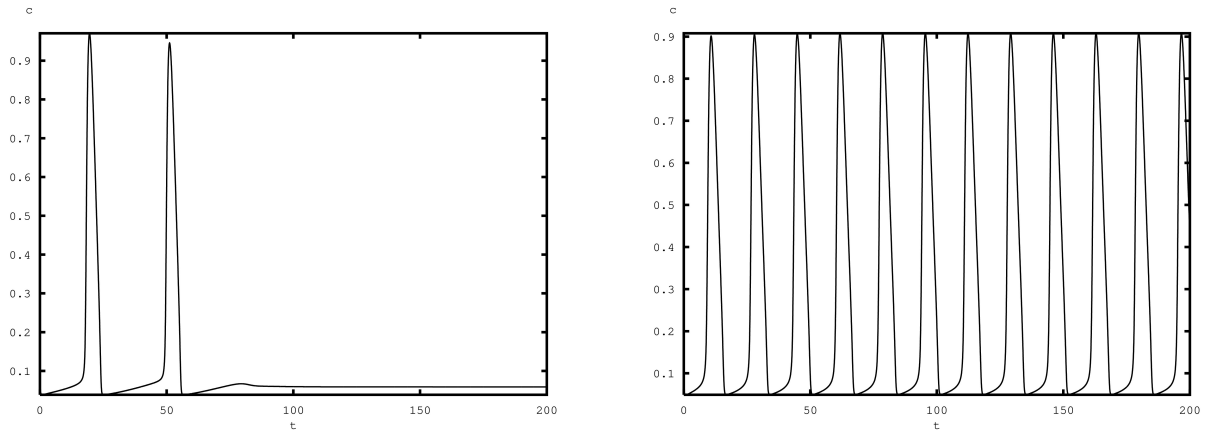

(a) (b)

Figure 3. These graphs Figure 3(a)-Figure 3(a) show the results of frequency modulation Ca^{2+} oscillations for IP_3 =0.5, r_L range 0.08 to 0.15 and k_{ER} =0.07

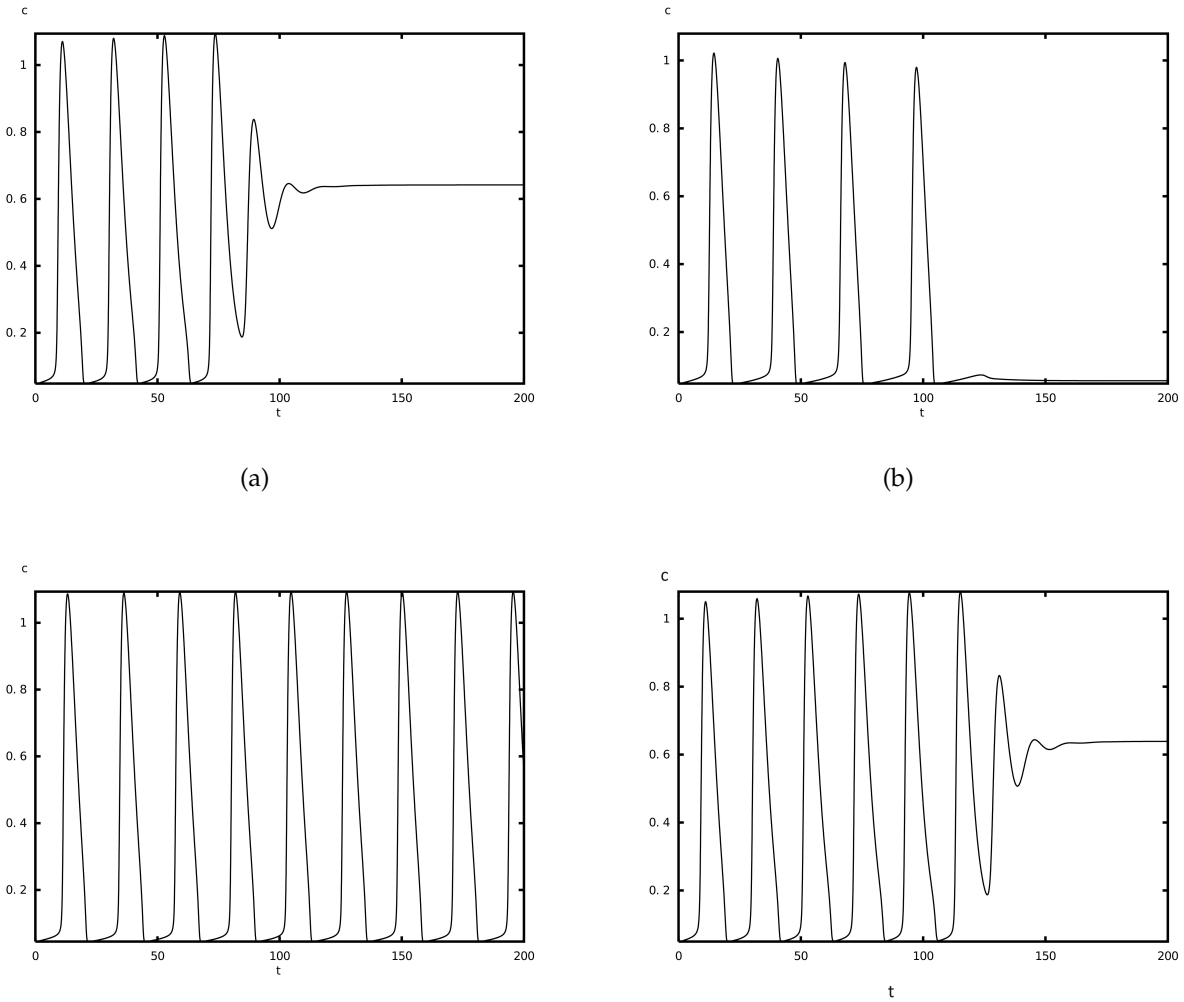

(a) (b)

(c) (d)

Figure 4. These graphs Figure 4(a)-Figure 4(d) show the results of frequency modulation Ca^{2+} oscillations IP_3=0.35, IP_3=0.32, IP_3=0.28, and IP_3=0.27, respectively, for $p = 0.13$ and $a = 1.15$

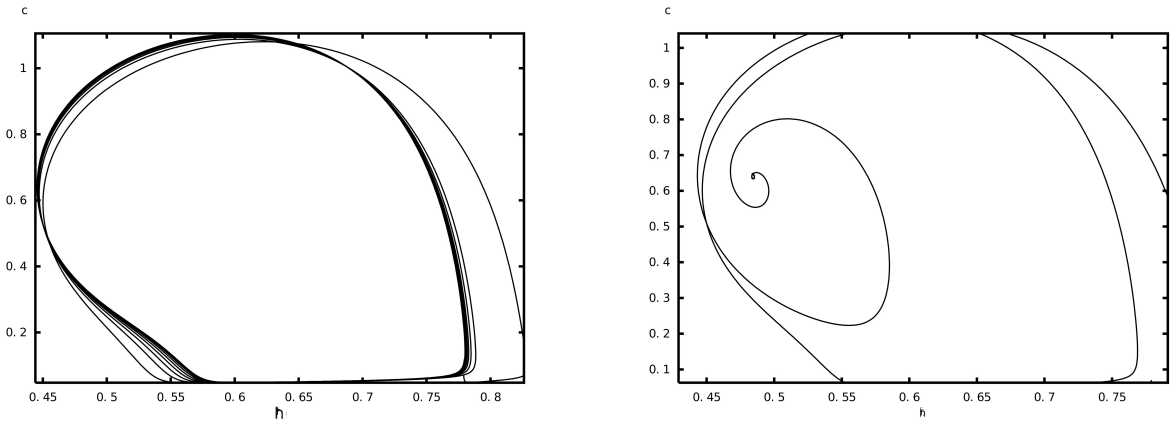

(a) (b)

Figure 5. The phase plane analysis diagram between Ca^{2+} and IP_3 fraction with distinct values of the parameters

4 Discussion

The cytoplasmic calcium level remains constant while the calcium dynamic is in equilibrium. The IP_3 readings are related to the stability of the calcium level. At low IP_3 values, Ca^{2+} oscillations are weakly stimulated; at higher IP_3 values, the modulation is altered by Ca^{2+} oscillations. As IP_3 increases in Figure 4, Ca^{2+} oscillations alter as Ca^{2+} concentration rises. The system eventually finds a stable state and loses its oscillation behavior at a certain value of IP_3. The experiment demonstrated that adding $A\beta$ directly increases Ca^{2+} dependent fluorescence, which is an indication of intracellular Ca^{2+} levels [30]. According to the findings, $A\beta$ does not directly bind with the IP_3 receptor; rather, it stimulates the synthesis of IP_3 through G-protein-mediated activation of PLC, which opens IP_3 receptors and causes intracellular Ca^{2+} liberation. As a result, even though IP_3 is digested in tens of seconds, IP_3 are actively activated in the presence of $A\beta$ and last for several minutes or hours. The Ca^{2+} oscillations appear and attain an equilibrium state for a specific range of IP_3. Figure 3 shows how Ca^{2+} oscillations alter modulation as r_L (Ca^{2+} leakage rate from ER) increases and reaches the steady-state at a greater level of Ca^{2+} concentration. At a specific value of r_L, the oscillation vanishes, and the concentration of Ca^{2+} achieves the steady-state. The Ca^{2+} oscillations appear and achieve an equilibrium state for a specific range 0.08 to 0.15 of r_L. Calcium dynamics is in equilibrium when the cytoplasmic calcium level is constant $(dc/dt = 0)$ and the percentage of inactive IP_3R remains constant $(dh/dt = 0)$. The calcium oscillations in Figure 4(a)-Figure 4(d) vary differently as IP_3^* (Baseline value of IP_3) decreases and eventually disappear when IP_3^* gets closer to a stable state. The calcium leakage rate from the ER causes the calcium concentration to stabilize. The calcium oscillation appears and reaches an equilibrium state for the $0.27 < IP_3^* < 0.36$. For a specific stimulation intensity, both the range and amplitude of calcium oscillations increase within the specified range. The highest value of the calcium responses in the amplitude modulation encodes the IP_3 level. It is closely related to how strongly the stimulus acts on the cell. Changes in IP_3 cause calcium responses in the frequency modulation and the information contained in those interspike intervals is encoded. IP_3^* must fluctuate dynamically under the influence of $A\beta$ in order to duplicate the reaction in Ca^{2+}. Examine the effect of membrane potential and consider model solutions for various IP_3^* concentration levels once $A\beta$ is fixed. In an experimental situation, IP_3^* can be photoreleased simultaneously throughout a cell. IP_3^* diffusion is constant and minimized under these conditions. The model can demonstrate

Ca^{2+} oscillations, indicative of various cell types, by varying the amount of IP_3^* accessible in the cytoplasm. These oscillation patterns are necessary for cells to maintain appropriate concentration gradients and recover homeostasis after a triggering event. In the presence of $A\beta$, model Ca^{2+} oscillations emerge and disappear due to transitions through amplitude modulations as IP_3^* grows. Dynamic transitions across (Figure 5) can account for both the increases in Ca^{2+} oscillations and the observed aberrant Ca^{2+} signals through phase-plane analysis. While there has been some accumulation of $A\beta$ in an AD environment, it is assumed that this quantity stays constant over the course of our simulation. $A\beta$ can accumulate to produce large amplitude oscillations and elevated steady-state values. A range of behaviors are displayed by the corresponding model solutions: aberrant Ca^{2+} signals, steady-state Ca^{2+} signals, and stable periodic solutions. An essential second messenger in the neurological system is intracellular Ca^{2+} regulation. The signaling pathways in neurons that govern neurotransmitter release, metabolism, gene expression, plasticity, development, proliferation, and cell death are known to be mediated by Ca^{2+}. Because of this, Ca^{2+} might be very important in the pathophysiology of AD. Unfortunately, understanding exactly how $A\beta$ affects various intracellular regulating mechanisms and components is challenging due to the complexity of Ca^{2+} signaling. Through the decoupling of specific components by various investigations, we can better comprehend intracellular Ca^{2+} signaling by combining these theories into a whole-cell computational model.

5 Conclusion

In the current study using the neuron-astrocyte model, the synaptic connection initiates diffusions of the gliotransmitters 2-AG and glutamates. The solution graphic shows how variable-parameter Ca^{2+} frequency and amplitude modulation of leak flow is impacted by mitochondria, NCX, and $A\beta$. The proposed model combines cell activation and intracellular signaling. A mathematical model is developed to accurately quantify the Ca^{2+}-mediated astrocytic exosome exocytosis in AD that is driven by Amyloid-beta. Our model indicates that increasing the amount of $A\beta$ can lead to aberrant signals and changes in homeostasis levels. A change in intracellular Ca^{2+} homeostasis can have an impact on the cascade of apoptotic signals. A comparison analysis was performed to quantify the effects of different components related to mitochondria, NCX, and $A\beta$ the leak fluxes on the calcium signaling process through the amplitude and frequency modulation. They do, however, transform into exosomes produced by astrocytes in AD, which have the potential to harm neurons. This computational model tracks the influence of numerous interrelated biological pathways, which can aid in our understanding of complicated cellular activity in an AD context.

Declarations

Ethical approval

The authors state that this research complies with ethical standards. This research does not involve either human participants or animals.

Consent for publication

Not applicable.

Conflicts of interest

The authors confirm that there is no competing interest in this study.

Data availability statement

Data availability is not applicable to this article as no new data were created or analyzed in this study.

List of abbreviations

Table 2. Abbreviations and their explanations

Abbreviations	Explanation
AD	Alzheimer's disease
CICR	Calcium-induced calcium release
ER	Endoplasmic reticulum
IP_3	Inositol triphosphate
IP_3R	Inositol triphosphate receptor
MAMs	Mitochondria associated membrane
MCU	Mitochondrial Ca^{2+} uniporter
mNCX	Mitochondrial Na^+ /Ca^{2+} exchangers
PLC	Phospholipase C
ROS	Reactive oxygen species
RYR	Ryanodine receptor
NCX	Na^+ /Ca^{2+} exchangers

Funding

The authors declare that they have never had any known competing financial interests or personal ties that may seem to have influenced the work revealed in this study.

Author's contributions

H.J.: Investigation. Data Curation, Conceptualization, Methodology, Software, Writing-Original draft preparation. B.K.J.: Supervision, Conceptualization, Methodology, Visualization, Validation, Writing-Reviewing and Editing. M.U.: Supervision, Writing-Reviewing and Editing. All authors have read and agreed to the published version of the manuscript.

Acknowledgements

The authors are highly thankful to all reviewers and editors for reviewing this article and giving valuable suggestions to improve the article.

References

[1] Ye, M. and Zuo, H. Stability analysis of regular and chaotic Ca^{2+} oscillations in astrocytes. *Discrete Dynamics in Nature and Society*, 2020, 1-9, (2020). [CrossRef]

[2] Wade, J.J., McDaid, L.J., Harkin, J., Crunelli, V. and Kelso, J.S. Bidirectional coupling between astrocytes and neurons mediates learning and dynamic coordination in the brain: a multiple modeling approach. *PloS One*, 6(12), e29445, (2011). [CrossRef]

[3] Dave, D.D. and Jha, B.K. Mathematical modeling of calcium oscillatory patterns in a neuron. *Interdisciplinary Sciences: Computational Life Sciences*, 13, 12-24, (2021). [CrossRef]

[4] Falcke, M., Or-Guil, M. and Bär, M. Dispersion gap and localized spiral waves in a model for intracellular Ca^{2+} dynamics. *Physical Review Letters*, 84(20), 4753, (2000). [CrossRef]

[5] Kalia, M., Meijer, H.G., van Gils, S.A., van Putten, M.J. and Rose, C.R. Ion dynamics at the energy-deprived tripartite synapse. *PLoS Computational Biology,* 17(6), e1009019, (2021). [CrossRef]

[6] Keener, J. and Sneyd, J. The Heart. In *Mathematical Physiology* (pp. 523-626). New York, NY: Springer, (2009). [CrossRef]

[7] Jha, B.K., Joshi, H. and Dave, D.D. Portraying the effect of calcium-binding proteins on cytosolic calcium concentration distribution fractionally in nerve cells. *Interdisciplinary Sciences: Computational Life Sciences,* 10, 674-685, (2018). [CrossRef]

[8] Jha, A. and Jha, B.K. Computational modelling of calcium buffering in a star shaped astrocyte. In Proceedings of the *2019 9th International Conference on Bioscience, Biochemistry and Bioinformatics (ICBBB)*, pp. 63-66, Singapore, (2019, January). [CrossRef]

[9] Dave, D.D. and Jha, B.K. 2D finite element estimation of calcium diffusion in Alzheimer's affected neuron. *Network Modeling Analysis in Health Informatics and Bioinformatics,* 10, 43, (2021). [CrossRef]

[10] Vatsal, V.H., Jha, B.K. and Singh, T.P. To study the effect of ER flux with buffer on the neuronal calcium. *The European Physical Journal Plus,* 138, 494, (2023). [CrossRef]

[11] Nadkarni, S. and Jung, P. Spontaneous oscillations of dressed neurons: a new mechanism for epilepsy?. *Physical Review Letters,* 91(26), 268101, (2003). [CrossRef]

[12] Lenk, K., Satuvuori, E., Lallouette, J., Ladrón-de-Guevara, A., Berry, H. and Hyttinen, J.A. A computational model of interactions between neuronal and astrocytic networks: the role of astrocytes in the stability of the neuronal firing rate. *Frontiers in Computational Neuroscience,* 13, 92, (2020). [CrossRef]

[13] Zuo, H. and Ye, M. Bifurcation and numerical simulations of Ca^{2+} oscillatory behavior in astrocytes. *Frontiers in Physics,* 8, 258, (2020). [CrossRef]

[14] Zhou, A., Liu, X. and Yu, P. Bifurcation analysis on the effect of store-operated and receptor-operated calcium channels for calcium oscillations in astrocytes. *Nonlinear Dynamics,* 97, 733-748, (2019). [CrossRef]

[15] Pankratova, E.V., Kalyakulina, A.I., Stasenko, S.V., Gordleeva, S.Y., Lazarevich, I.A. and Kazantsev, V.B. Neuronal synchronization enhanced by neuron–astrocyte interaction. *Nonlinear Dynamics,* 97, 647-662, (2019). [CrossRef]

[16] Oku, Y., Fresemann, J., Miwakeichi, F. and Hülsmann, S. Respiratory calcium fluctuations in low-frequency oscillating astrocytes in the pre-Bötzinger complex. *Respiratory Physiology & Neurobiology,* 226, 11-17, (2016). [CrossRef]

[17] Naji, R. and Abdulateef, B. The dynamics of model with nonlinear incidence rate and saturated treatment function. *Science International,* 29(6), 1223-1236, (2017).

[18] Li, J.J., Du, M.M., Wang, R., Lei, J.Z. and Wu, Y. Astrocytic gliotransmitter: diffusion dynamics and induction of information processing on tripartite synapses. *International Journal of Bifurcation and Chaos,* 26(08), 1650138, (2016). [CrossRef]

[19] Matrosov, V.V. and Kazantsev, V.B. Bifurcation mechanisms of regular and chaotic network signaling in brain astrocytes. *Chaos: An Interdisciplinary Journal of Nonlinear Science,* 21(2), 023103, (2011). [CrossRef]

[20] Faramarzi, F., Azad, F., Amiri, M. and Linares-Barranco, B. A neuromorphic digital circuit for neuronal information encoding using astrocytic calcium oscillations. *Frontiers in Neuroscience,* 13, 998, (2019). [CrossRef]

[21] Singh, T. and Adlakha, N. Numerical investigations and simulation of calcium distribution in the alpha-cell. *Bulletin of Biomathematics,* 1(1), 40-57, (2023). [CrossRef]

[22] Joshi, H. and Jha, B.K. Chaos of calcium diffusion in Parkinson's infectious disease model and treatment mechanism via Hilfer fractional derivative. *Mathematical Modelling and Numerical Simulation with Applications,* 1(2), 84-94, (2021). [CrossRef]

[23] Nakul, N., Mishra, V. and Adlakha, N. Finite volume simulation of calcium distribution in a cholangiocyte cell. *Mathematical Modelling and Numerical Simulation with Applications,* 3(1), 17-32, (2023). [CrossRef]

[24] Naik, P.A. Modeling the mechanics of calcium regulation in T lymphocyte: a finite element method approach. *International Journal of Biomathematics,* 13(05), 2050038, (2020). [CrossRef]

[25] Naik, P.A. and Pardasani, K.R. Finite element model to study calcium signalling in oocyte cell. *International Journal of Modern Mathematical Sciences,* 15(01), 58-71, (2017).

[26] Naik, P.A. and Pardasani, K.R. Three-dimensional finite element model to study calcium distribution in oocytes. *Network Modeling Analysis in Health Informatics and Bioinformatics,* 6, 16, (2017). [CrossRef]

[27] Joshi, H., Yavuz, M. and Stamova, I. Analysis of the disturbance effect in intracellular calcium dynamic on fibroblast cells with an exponential kernel law. *Bulletin of Biomathematics,* 1(1), 24-39, (2023). [CrossRef]

[28] Naik, P.A., Eskandari, Z. and Shahraki, H.E. Flip and generalized flip bifurcations of a two-dimensional discrete-time chemical model. *Mathematical Modelling and Numerical Simulation with Applications,* 1(2), 95-101, (2021). [CrossRef]

[29] Marambaud, P., Dreses-Werringloer, U. and Vingtdeux, V. Calcium signaling in neurodegeneration. *Molecular Neurodegeneration,* 4, 20, (2009). [CrossRef]

[30] Latulippe, J., Lotito, D. and Murby, D. A mathematical model for the effects of amyloid beta on intracellular calcium. *PLoS One,* 13(8), e0202503, (2018). [CrossRef]

[31] Manninen, T., Havela, R. and Linne, M.L. Reproducibility and comparability of computational models for astrocyte calcium excitability. *Frontiers in Neuroinformatics,* 11, 11, (2017). [CrossRef]

[32] Schampel, A. and Kuerten, S. Danger: high voltage-the role of voltage-gated calcium channels in central nervous system pathology. *Cells,* 6(4), 43, (2017). [CrossRef]

[33] Grubelnik, V., Larsen, A.Z., Kummer, U., Olsen, L.F. and Marhl, M. Mitochondria regulate the amplitude of simple and complex calcium oscillations. *Biophysical Chemistry,* 94(1-2), 59-74, (2001). [CrossRef]

[34] Jha, B.K., Jha, A. and Adlakha, N. Three-dimensional finite element model to study calcium distribution in astrocytes in presence of VGCC and excess buffer. *Differential Equations and Dynamical Systems,* 28, 603-616, (2020). [CrossRef]

[35] Cataldi, M. The changing landscape of voltage-gated calcium channels in neurovascular disorders and in neurodegenerative diseases. *Current Neuropharmacology,* 11(3), 276-297, (2013). [CrossRef]

[36] Gao, H., Liu, L. and Chen, S. Simulation of Ca^{2+} oscillations in astrocytes mediated by amyloid beta in Alzheimer's disease. *BioRxiv,* 2020-03, (2020). [CrossRef]

[37] Liu, L., Gao, H., Li, J. and Chen, S. Probing microdomain Ca^{2+} activity and synaptic transmission with a node-based tripartite synapse model. *Frontiers in Network Physiology,* 3, 1111306, (2023). [CrossRef]

[38] Zeng, S., Li, B., Zeng, S. and Chen, S. Simulation of spontaneous Ca^{2+} oscillations in astrocytes mediated by voltage-gated calcium channels. *Biophysical Journal*, 97(9), 2429-2437, (2009).

[39] Ermentrout, B. and Mahajan, A. Simulating, analyzing, and animating dynamical systems: a guide to XPPAUT for researchers and students. *Applied Mechanics Reviews*, 56(4), B53, (2003). [CrossRef]

Mathematical Modelling and Numerical Simulation with Applications (MMNSA)
(https://dergipark.org.tr/en/pub/mmnsa)

How to cite this article: Hemlata Jethanandan, H., Jha, B.K. & Ubale, M. (2023). The role of calcium dynamics with amyloid beta on neuron-astrocyte coupling. *Mathematical Modelling and Numerical Simulation with Applications*, 3(4), 376-390. https://doi.org/10.53391/mmnsa.1398320